1959

Heat transfer characteristics of screen matrices at low Reynolds numbers.

St. Ville, Edward L.

Monterey, California: U.S. Naval Postgraduate School

HEAT TRANSFER CHARACTERISTICS OF SCREEN MATRICES AT LOW REYNOLDS NUMBERS

EDWARD L. ST. VILLE

HEAT TRANSFER CHARACTERISTICS OF SCREEN MATRICES AT LOW REYNOLDS NUMBERS

* * * * * *

Edward L. St. Ville

HEAT TRANSFER CHARACTERISTICS OF SCREEN MATRICES AT LOW REYNOLDS NUMBERS

by

Edward L. St. Ville

Lieutenant, United States Navy

Submitted in partial fulfillment of
the requirements for the degree of

MASTER OF SCIENCE
IN
MECHANICAL ENGINEERING

United States Naval Postgraduate School
Monterey, California

1959

HEAT TRANSFER CHARACTERISTICS

OF SCREEN MATRICES AT LOW REYNOLDS NUMBERS

by

Edward L. St. Ville

This work is accepted as fulfilling

the thesis requirements for the degree of

MASTER OF SCIENCE

IN

MECHANICAL ENGINEERING

from the

United States Naval Postgraduate School

ABSTRACT

The convective heat transfer characteristics of six screen matrices with a range of porosity from 0.602 to 0.832 are presented. The characteristics were investigated over a Reynolds number range of 0.1 to 10, based on hydraulic diameter. The data was obtained by passing air through a 6 in. diameter woven screen matrix composed of three stacked screens.

The heat transfer data was obtained by use of the transient technique developed by G. L. Locke at Stanford University. Temperature-time history of the downstream air temperature is used to determine the maximum slope of the experimental cooling curve. From a plot of maximum slope versus NTU of the generalized cooling curve, which is a unique solution for this type of cooling, an evaluation of the experimental NTU is possible. With the NTU thus determined, the experimental value of the thermal conductance coefficient, h, is readily obtained.

The present data is an extension of existing data and was obtained using the same type of matrices but with a slightly different technique and over a lower range of Reynolds numbers. The present technique involves heating the screen matrix to a uniform temperature and introducing the screens into a stream of air entering at a uniformly lower temperature. The temperature-time history of the downstream air is recorded and available for analysis.

Application of the present data is thought to be useful in transpiration cooling of environmental chambers subjected to an external heat source.

ACKNOWLEDGEMENTS

The author wishes to thank P. Pucci, Assistant Professor of Mechanical Engineering for his guidance and under whose direction this work was carried out. My thanks also to C. Howard, Assistant Professor of Mechanical Engineering for his aid and suggestion on various problems encountered in this project.

The assistance of R. Kennicott and J. Beck in fabricating and assembling the equipment used in this work is acknowledged.

Particular thanks is given to the Cambridge Wire Cloth Co., Cambridge, Maryland and to the Colorado Fuel and Iron Corp., Buffalo, New York for their contribution of the wire screen matrices used in this investigation.

TABLE OF CONTENTS

LIST OF ILLUSTRATIONS

LIST OF TABLES

TABLE OF SYMBOLS AND ABBREVIATIONS

English Letter Symbols

A - heat transfer area, ft^2

A_f - matrix free flow area, $A_f = \alpha A_t$, ft^2

A_f' - free flow area of a single screen or a perfectly packed screen matrix, $A_f' = \alpha A_t$, ft^2

A_t - matrix frontal area, ft^2

c_f - specific heat at constant pressure, BTU/(lbm ^oF)

c_s - specific heat of solid phase, BTU/lbm ^oF

C - thermal capacity rate, $C = wc_p$, BTU/(hr ^oF)

D - Diameter, ft

D_h - hydraulic diameter, $D_h = 4 r_h$, ft

D_h' - hydraulic diameter of single screen or of a perfectly packed screen matrix, $D_h' = 4 r_h'$, ft

G - mass velocity, lbm/(hr ft^2)

G_i - mass velocity based on matrix free flow area, $G_i = w_f/A_f$, lbm/(hr ft^2)

G_i' - mass velocity based on free flow area of a single screen or of a perfectly packed screen matrix, $G_i' = w_f/A_f'$, lbm/(hr ft^2)

h - unit conductance for convective heat transfer, BTU/(hr ft^2 ^oF)

k - thermal conductivity, BTU/(hr ft^2 ^oF/ft)

L - flow length of matrix, ft

n - number of screens in matrix

q - heat transfer rate, BTU/hr

r_h - hydraulic radius, $r_h = \alpha/\beta$, ft

r_h' - hydraulic radius of a single screen or of a perfectly packed screen matrix, $r_h' = \alpha'/\beta'$, ft

t - temperature, ^oF

T - temperature, ^oR

V - velocity of fluid based on frontal area, ft/sec

V_i - velocity of fluid based on free flow area, ft/sec

V_i' - velocity of fluid based on free flow area of a single screen or of a perfectly packed screen matrix, ft/sec

w_f - mass flow rate of fluid, lbm/hr

W_f - mass of fluid contained in pores of matrix, lbm

W_s - mass of solid in matrix, lbm

x - distance from entrance of matrix to a given cross section measured in the direction of flow, ft

Greek Letter Symbols

α - porosity, α = volume of voids/ total matrix volume, nondimensional

α' - porosity of a single screen or of a perfectly packed screen matrix, nondimensional

β - heat transfer area per unit volume of matrix, ft^{-1}

β' - heat transfer area per unit volume of a single screen of or a perfectly packed screen matrix, ft^{-1}

θ - time, hrs

μ - viscosity, lbm/(hr ft)

ρ - mass density, lbm/ ft^3

Dimensionless Groupings

NTU - number of heat transfer units, $NTU = hA/(w_f c_f)$

N_{Pr} - Prandtl number, $N_{Pr} = c_f \mu_f / k_f$

N_{Re} - Reynolds number, $N_{Re} = D_h G_i / \mu_f$

N_{Re}' - Reynolds number employed for screen matrices, $N_{Re}' = D_h' G_i' / \mu_f$

N_{St} - Stanton number, $N_{St} = h/G_i c_f$

N_{St}' - Stanton number employed for screen matrices, $N_{St}' = h/G_i' c_f$

τ - generalized time variable, $\tau = hA/W_s c_s(\theta - W_f x/w_f L)$

z - generalized position variable, $z = (hA/w_f c_f)\, x/L$

Subscripts

a - refers to atmospheric conditions

f - refers to the fluid phase

i - refers to matrix initial state

s - refers to the solid phase

1 - refers to the fluid state upstream of the matrix

2 - refers to the fluid state downstream of the matrix

1. Introduction.

In this study, porous media is defined as a solid matrix possessing a high ratio of void surface area to bulk volume ft^2/ ft^3, and a void geometry which permits flow of gas or liquid through the matrix. The term porous media is used throughout, to refer only to those random homogenous configurations which result in three dimensional flows, with frequent contractions and expansions.

In the past, heat transfer characteristics of porous media have been of interest primarily in the study of the flow of oil and water through underground formations, the flow of gases through blast furnace charges, and the flow through the granular packing used in absorption and stripping columns and catalyst beds. Other applications of more recent interest are found in:

a. Periodic-flow, regenerative type heat exchangers

b. Nuclear reactors

c. Boundary layer control for air foils

d. Transpiration or sweat cooling of environmental enclosures.

In regenerative heat exchangers the energy transfer from the hot to cold fluid is accomplished first by transfer from the hot fluid to the solid matrix followed later by a transfer from the matrix to a cold fluid. Thus, the matrix is alternately heated and cooled either by periodic movement of the solid from the hot to cold streams and back again, as in rotary-type regenerative exchangers (Ljunstrom air-preheaters), or by sequential valving of the hot and cold gas streams through two solid matrices in parallel. In the past, types of matrices used were of the nature of brick checkerwork or packed corrugated plates -- constructions which do not possess a very large transfer area per unit volume. As an

illustration of the wide variance in the degree of compactness of various matrices the following tabulation was prepared.

MATRIX	APPROXIMATE AREA/UNIT VOLUME ft^2/ft^3
1. Brick Checkerwork	0.8
2. Rod banks, rod dia. - 0.375 in. $x_\ell^* = 1$ $x_t^* = 2$	51
3. Corrugated plates (Used in Ljungstrom heaters)	150
4. Sphere Beds	
a. 1/4 in. spheres	170
b. 1/16 in. spheres	690
c. 1/32 in. spheres	1380
5. Packed Wire Screens	
a. 5 mesh	190
b. 20 mesh	760
c. 50 mesh	1900
d. 300 mesh	11,400

*x_ℓ - Ratio of longitudinal pitch to tube diameter for flow across banks of circular tubes, dimensionless.

*x_t - Ratio of transverse pitch to tube diameter for flow across banks of circular tubes, dimensionless.

Nuclear reactors for electric power generation consist essentially of a solid matrix in which the thermal energy created by fission is transferred as heat to a working substance passing through it. Thus the possibility of making the fuel in the form of a porous medium through which to pass the cooling fluid should be considered. The principle advantage being that of high heat transfer effectiveness which would enable the use of a gaseous medium for a primary coolant. In addition, if porous solids are practical for this application it may be possible to reduce the volume

and the overall bulk and mass of the system.

The feasibility of using porous media for boundary layer control has come to the fore primarily due to the development of sintered metals. Sintered metals are an excellent example of porous media, the area density being of the order of the 300 mesh screens. Interest has centered principally in the use of area suction to delay boundary layer transition and thus take advantage of the lower drag which accompanies laminar flow at high Reynolds numbers.

Recently attention has been focused on the possible use of porous media as an enclosure for constant temperature environmental chambers. The problem of maintaining an enclosed area at a temperature within, such that it is suitable for human existance, when such an enclosure is subjected to extreme outside temperatures, has been encountered in the aircraft industry. Pilots who will experience atmospheric reentry frictional heating in the proposed new aircraft, must be provided with a cockpit which will remain at "shirt sleeve temperature". The use of porous walls has been proposed for the cockpit lining, with facilities for inducing air flow outward through the walls, thus cooling an otherwise radiant heat emitter. This system is believed to be an excellent solution to this problem. One primary advantage being that of great weight saving in air conditioning equipment, which would otherwise be required.

These applications suggest the desireability of an increased program of study of the convective heat transfer behavior in porous solids. Although some work has been started in this country and more in Great Britian, there still remains a paucity of data useful for design at the present time. The principal reason for this lack, is the difficulty in accurate experimentation. The possibilities of using porous media for

transpiration cooling at low flow rates, provided the motive for the present investigation.

2. Objectives.

a. Develop a testing technique to determine the basic convective heat transfer data for the flow of air through wire screen matrices, at low Reynolds numbers.

b. Obtain the heat transfer data for screen matrices over the Reynolds number range 0.1 to 10, based on hydraulic diameter.

c. Summarize previous work in the field of porous media and to compare the previous results with the results of the present study.

The work done in developing the analytical solution and method used in the present work is fully described by Locke in Reference (1)*.

*Numbers in parentheses refer to Bibliography on page of this paper.

3. Summary of Contents.

A review of previous investigation procedures is presented first, followed by a discussion of the reasons this investigator chose the particular method used. The method of presenting the heat transfer data is then discussed. Presentation of the data will be made graphically as well as tabularly. Graphic representation is plotted as Reynolds number, N_{Re}', as later defined, versus $N_{St}'N_{Pr}^{2/3}$. The range of Reynolds numbers covered is from 0.1 to 10.

A complete description of all the matrices tested is discussed. Details of each of the six types of woven wire screens are given, along with details of the matrices assembled from these screens. A complete description of the test apparatus and test program is then presented.

Heat transfer data for wire screen matrices, obtained by Coppage (2), are compared to the present results. Based on the results of this investigation recommendations for future work are made.

4. Review of Previous Work

The theoretical analysis of the transient heat transfer behavior of a porous medium was first presented by Schumann (4) in 1929. The porous solid is considered to be homogeneous and initially at a uniform temperature. A fluid at the same temperature as the solid, is flowing through the medium. At a certain instant the temperature of the entering fluid is assumed to change to a higher or lower temperature. The problem is then to find the temperature of the fluid and the solid as functions of time and position in the matrix.

The analytical solution for the convective heat transfer coefficient of porous solids, requires that the following idealizations, initial conditions and boundary conditions be satisfied.

Idealizations:

1. The fluid specific heat and viscosity are constant
2. The flow is constant
3. The porous solid is homogenous
4. The thermal conductivity of both the fluid and solid is infinite perpendicular to the flow and zero parallel to the flow.

Initial and Boundary Conditions:

1. Initially the core is at a uniform temperature
2. At time $\theta = 0$, the temperature of the incoming fluid changes instantaneously.
3. No heat passes the core boundaries.

An energy balance on a fluid element within the porous medium yields

$$dq = w_f c_f \frac{\partial t_f}{\partial x} dx + A_f \rho_f c_f \frac{\partial t_f}{\partial \theta} dx \qquad (1)$$

The rate equation expressing the convective heat transfer between the porous medium and fluid is

$$dq = h(t_s - t_f)\lambda\, dx \tag{2}$$

where λ = total perimeter of the flow tube at a given cross section.

An energy balance on the porous medium yields

$$dq = -A_s \rho_s c_s \frac{\partial t_s}{\partial \theta} dx \tag{3}$$

Introducing the variables τ and z for the variables θ and x respectively, where

τ = generalized time variable

$$\tau = \frac{hA}{W_s c_s}\left(\theta - \frac{W_f x}{w_f L}\right)$$

z = generalized position variable

$$z = \left(\frac{hA}{w_f c_f}\right)\frac{x}{L}$$

= NTU, when x = L

and observing that the thermal capacity of the porous medium is much greater than the thermal capacity of the fluid within the porous medium, that is, $W_s c_s \gg W_f c_f$, equations (1) and (2) combine to yield

$$\frac{\partial t_f}{\partial z} = t_s - t_f \tag{4}$$

and equations (2) and (3) combine to yield

$$\frac{\partial t_s}{\partial \tau} = t_f - t_s \tag{5}$$

The boundary and initial conditions are:

$$t_f(0,\tau) = t_{f_1} \tag{6}$$

$$t_f(z,0) = t_i + (t_{f_1} - t_i)\, e^{-z} \tag{7}$$

The solutions to equations (4) and (5) together with the boundary conditions are found to be

$$\frac{t_f - t_i}{t_{f_1} - t_i} = e^{-(z+\tau)} \sum_{n=0}^{\infty} \tau^n \frac{d^n}{d(z\tau)^n} \left[J_o (2i\sqrt{z\tau}) \right] \tag{8}$$

$$= 1 - e^{-(z+\tau)} \sum_{n=1}^{\infty} z^n \frac{d^n}{d(z\tau)^n} \left[J_o (2i\sqrt{z\tau}) \right] \tag{9}$$

$$\frac{t_s - t_i}{t_{f_1} - t_i} = e^{-(z+\tau)} \sum_{n=1}^{\infty} \tau^n \frac{d^n}{d(z\tau)^n} \left[J_o (2i\sqrt{z\tau}) \right] \tag{10}$$

$$= 1 - e^{-(z+\tau)} \sum_{n=0}^{\infty} z^n \frac{d^n}{d(z\tau)^n} \left[J_o (2i\sqrt{z\tau}) \right] \tag{11}$$

Schumann's solution was first used as the basis for a transient testing technique by Furnas (5) in 1932 when he passed air through granular beds. The fluid temperature was measured at the exit of the matrix where z = NTU. Furnas compared his experimental data with Schumann's theoretical constant z curves. The z value of the theoretical curve which fitted the experimental data was considered as the NTU of the matrix, and thereby the convection conductance h was evaluated. His work was limited in the Reynolds number range from 300 to 2000, based on the hydraulic diameter.

Saunders and Ford (6) used essentially the same method in 1940 to obtain the heat transfer coefficient, h when air was passed through beds of spherical balls with porosity = 0.38. Tests were made at Reynolds numbers from 145 to 290, based on hydraulic diameter. Their results indicated a constant Stanton number, and with the assumption of $N_{Pr} = 0.74$ for air, the following equation may be obtained from their work:

$$N_{St} N_{Pr}^{2/3} = 0.05$$

Lof and Hawley (7) used the same transient technique in 1948 to examine four sizes of gravel in beds over the Reynolds number range 5 to 500, based on hydraulic diameter. Their results indicated a large discrepancy existing between available data and even in the same group. The reason for this discrepancy, according to Coppage (2), may be due to the heat losses to the matrix boundaries and to other thermal capacitances in the experimental system.

Romie (3) used the same transient technique in passing air through a screen matrix in 1948. He tested two wire screen matrices in which the screens were separated 1/32 inch, and covered the Reynolds number range from 20 to 500, based on hydraulic diameter and the mass velocity, based on free flow area.

In evaluating the heat transfer coefficients, Romie plotted his data in the form $(t_{f_1} - t_{f_2}) / (t_{f_1} - t_i)$ versus τ/NTU and measured the area under the curves up to a given value of τ/NTU. From Schumann's theoretical curves of $(t_{f_1} - t_f) / (t_{f_1} - t_i)$ versus τ/z the area under the curves was obtained as a function of NTU, and the experimental NTU could thus be determined.

Locke (1) in 1950 developed an improved method of evaluation of the experimental NTU from the theoretical curves to eleminate the possible error introduced by a displacement of the experimentally determined heating curve either horizontally or vertically. In his method only the maximum slopes of the theoretical and experimental curves need be compared. He derived an expression for the slope of the generalized heating curve, $(t_f - t_i) / (t_{f_1} - t_i)$ versus τ/z, finding that

$$\frac{d\left(\frac{t_{f_2} - t_i}{t_{f_1} - t_i}\right)}{d\left(\frac{\tau}{NTU}\right)} = \frac{NTU^2}{\sqrt{NTU \cdot \tau}} \left[-i\, J_1\left(2i\sqrt{NTU \cdot \tau}\right)\right] e^{-(NTU+\tau)} \qquad (12)$$

for the position $x = L$, at which $z = NTU$ and $t_f = t_{f_2}$. From this it was found that the maximum slope of the generalized heating curve is a unique function of NTU. Therefore with this unique function available, only the maximum slope of the experimental cooling curve need be determined. From the plot of maximum slope versus NTU, the NTU for the experimental curve is obtained and $\underline{h}$ is easily obtained from the relationship $NTU = hA/w_f c_f$.

Saunders and Smoleniec (8) tested three screen matrices in 1951 in the Reynolds number range 20 to 1000, based on hydraulic diameter. They passed air through the matrix, and the convective heat transfer coefficient was evaluated by comparing the maximum slopes of the theoritical and experimental generalized curves. They presented the heat transfer data of screen matrices in a plot of N_{Nu} versus N_{Re}. When the curve was compared to the results of N_{Nu} versus N_{Re} for flow normal to a single cylinder, the performance was quite similar.

Coppage (2) tested six screen matrices in 1952 by using the same transient technique developed by Locke (1). He covered the Reynolds number range 10 to 1000. Air was used as the working fluid. The porosities of the screen matrices tested were from 0.602 to 0.832, which covers almost the whole range of porosities of all square mesh, close packed screen matrices. In addition, he also tested a matrix of packed spheres. The diameter of the spheres was 0.0818 in., and the porosity of the sphere matrix was 0.390.

This investigation has extended Coppage's data to the Reynolds number range 0.1 to 10. The data obtained is plotted as $N_{St}' N_{Pr}^{2/3}$ versus N_{Re}' and is compared to Coppage's data at the overlap region of N_{Re}' approximately equal to 10. Coppage's data is replotted as $N_{St}' N_{Pr}^{2/3}$ vice $N_{St}' N_{Pr}$ for comparison purposes.

5. Advantages and Disadvantages of Transient Method.

The transient method as used by Furnas (5) and Saunders and Ford (6) is based on the solution of Schumann's (4) transient problem as outlined above. A porous solid initially at a uniform temperature is heated or cooled by a fluid passing through it, and $\frac{t_{f_2} - t_i}{t_{f_1} - t_i}$ is plotted as a function of

$$\frac{w_f c_f}{W_s c_s}\left[\theta - \frac{W_f}{w_f}\right].$$ Since at $x = L$, $\frac{\tau}{z} = \frac{\tau}{NTU} = \frac{w_f c_f}{W_s c_s}\left[\theta - \frac{W_f}{w_f}\right]$;

this curve can be compared to the family of theoretical curves of $(t_f - t_i) / (t_{f_1} - t_i)$ versus τ/z with z as a parameter. The analytical curve which matches the experimental one will then give the value of NTU from which h can be computed. There are three advantages to this method, (1) the fluid temperature only need be measured, (2) a core would be simple to construct and (3) any type of porous solid can be tested. A disadvantage of this comparison method is the difficulty encountered in the calculation of the theoretical curves. Calculation of these curves involves the evaluation of an infinite series for each point and the number of terms which must be taken to obtain a good approximation increases as NTU increases.

As indicated above, Romie (3) obtained the area under his curves and compared them to the areas under the analytical solution curves. From the plot of the area as a function of NTU, the experimental NTU could be determined and thus h could be obtained. As pointed out by Locke (1) both these methods have the disadvantage that a displacement of the experimentally determined heating curve either horizontally or vertically introduces errors in the results.

In the method as developed by Locke (1) only the maximum slope of

the experimental plot of $(t_{f_2} - t_i) / (t_{f_1} - t_i)$ versus τ/NTU need be determined. Since the maximum slope of the generalized heating curve is a unique function of NTU, the experimental NTU value can easily be obtained from the curve. This function from equation (12) is reproduced in Figure 8. A further advantage of the maximum slope technique is that the experimental range which can be conveniently covered is widened. In this method, actually, a premium is placed on a large NTU and τ in the analysis of the experimental data. Figure 9 is a plot of (% error in $\underline{h}$) / (% error in max. slope) versus NTU. This plot shows the obvious advantage of a large NTU and suggests the avoidance of NTU in the range 1 thru 4 where the inflection point of equation (12) occurs. This did not pose a significant disadvantage in this investigation since porous media tend to have NTU greater than 5 because of large heat transfer area. In addition the flow rates used were sufficiently low in all cases to insure values higher than NTU = 5. The chief disadvantage in this method is that any error in the experimentally determined maximum slope, is magnified in the corresponding value of NTU. However, a comparable disadvantage is also inherent in the other methods also.

Thus for the usual porous media, with it's high NTU, the single blow transient method with the maximum slope technique is considered the most desirable and is used in the determination of data in this report.

The method requires more care than the steady state technique to approach the idealizations and initial and boundary conditions of the theoretical analysis, which are restated below.

Idealizations

1. The fluid specific heat and viscosity are constant
2. The flow is steady
3. The porous solid is homogenous

4. The thermal conductivity of both fluid and solid is zero in the direction of flow and is infinite within the fluid and solid in the direction normal to the flow. Effectively all the convective resistance is lumped at the fluid-solid interface.

Since the fluid used is air, the first idealization can be approached if temperature differences are kept small. For instance, if the maximum air temperature variation is from 80°F to 100°F, the maximum deviation from the arithmetic average will be plus or minus 1.5% in viscosity and negligible in specific heat.

The second and third idealizations can be approached by careful design and selection of equipment, and by discreet selection of the porous solid to be tested. The fourth idealization, however, can be approached only by correct core design. As pointed out by Locke (1) and Coppage (2), this poses no problem since heat transfer in the flow direction is ordinarily very small in the fluid and may be made negligible in the solid by interrupting the solid material. In the direction normal to the flow, the conduction paths in both fluid and solid are usually small so that the effect is that of low thermal resistance within the solid relative to the resistance between them.

Initial and Boundary Conditions

1. Initially the core is at a uniform temperature.
2. At time $\theta = 0$, the temperature of the fluid flowing past the screens changes instantaneously.
3. No heat passes the core boundaries.

The first condition is achieved satisfactorily if suitable precautions are taken to insure uniform heating of the screens at temperature other

than ambient. The second condition requires some method of rapidly introducing the heated screens into the flow stream of constant temperature ambient air. The problem of heat loss to the walls of the approach ducting, as encountered by Coppage (2), is avoided in this particular technique, in that ambient air is flowing thru the test duct and thus remains constant up until the time it encounters the heated matrix. The third condition can only be minimized by careful design of the matrix holder. Since the screens are heated while contained in the matrix holding device, which has a certain thermal capacitance, an unavoidable transfer of heat from the holder to the screens will result as they are cooled. However this effect is minimized in the design of the matrix holder.

Additional consideration of the foregoing requirements was made by Locke (1) and the design criteria established.

Briefly, the experimental method used in obtaining the heat transfer data is as follows: the matrix, heated initially to a uniform temperature, is cooled by the fluid which enters at a constant, lower temperature. The temperature-time history of the fluid leaving the matrix is recorded during the cooling process. The maximum slope of the "cooling curve" is compared to that of the theoretical cooling curve. From a plot of the maximum slope of the theoretical cooling curve versus NTU, the NTU corresponding to the maximum slope of the experimental cooling curve can be obtained. Thus, in this manner the heat transfer unit conductance can be obtained.

6. Method of Presentation of Results.

Through the dimensional analysis of the problem of heat transfer to a porous medium as developed by Coppage (2), it is seen that a definition for flow diameter, other than that normally used for flow thru pipes, will be necessary. In comparing two geometrically similar media it is clear that only one diameter is needed to define the relative sizes of the flow passages. From the description of the porous media used in this investigation and previous investigations, it is seen that all such media have flow passages which are at least qualitatively similar, in that they all have a random, three-dimensional character and involve many contractions and expansions. Thus in comparing various porous media a single dimension can provide a very good measure of the relative sizes of the flow passages. One very logical choice of a dimension is based on the familiar concept of a hydraulic radius. The hydraulic radius of a prismatical flow passage is defined as

$$r_h = \frac{\text{flow passage cross-sectional area}}{\text{flow passage wetted perimeter}}$$

If numerator and denominator are each multiplied by the length of the flow passage, then

$$r_h = \frac{\text{flow passage volume}}{\text{flow passage surface area}}$$

This latter form now provides a possible basis for defining a suitable average hydraulic radius in a porous medium. Therefore, this definition will now be used for screen matrices even though the flow passages are not cylindrical. The relationship is valid since it is merely a defined quantity.

In order to get the average r_h of all passages in the matrix, one can extend the above definition to

$$r_h = \frac{\text{Total flow passage volume}}{\text{Total flow passage surface area}}$$

If both numerator and denominator are divided by the total volume of the matrix, the result is

$$r_h = \frac{\text{Total void volume/total matrix volume}}{\text{Total void surface area/total matrix volume}}$$

$$= \frac{\alpha}{\beta}$$

where

$$\alpha = \frac{\text{Total volume of voids}}{\text{Total volume of matrix}} = \text{POROSITY}$$

$$\beta = \frac{\text{Total surface area of voids}}{\text{Total volume of matrix}}$$

The average flow passage diameter is the conventional hydraulic diameter

$$D_h = 4r_h$$

Now in order to establish an average mass velocity, an average free flow cross-sectional area, A_f, may be defined such that

$A_f L$ = Volume of flow passages in matrix

= Volume of voids in matrix

If both sides of the equation are divided by the total matrix volume we get

$$A_f = \alpha A_t$$

A_t = Total frontal area of the matrix

Therefore, the average mass velocity

$$G_i = \frac{w_f}{A_f} = \frac{w_f}{\alpha A_t} = \frac{G}{\alpha}$$

Likewise for the average flow velocity

$$V_i = \frac{w_f}{\rho_f A_f} = \frac{w_f}{\alpha \rho_f A_f} = \frac{V}{\alpha}$$

The above definitions are based upon the total matrix dimensions, and therefore some modifications must be made in order to adapt these definitions to a single screen of the matrix. To accomplish this, the following

definitions will be made.

α' = Porosity of a single screen

β' = Surface area / unit volume for a single screen

Therefore

$r_h' = \frac{\alpha'}{\beta'}$ hydraulic radius of a single screen

$A_f' = \alpha' A_t$

$G_i' = w_f/A_f' = G/\alpha'$

$V_i' = w_f/\rho_f A_f = V/\alpha'$

Based upon these new definitions then, the dimensionless groupings for single screen matrices are:

$$(h/G_i' c_f) = \phi\ (D_h' G_i'/\mu_f;\ c_f \mu_f/k_f\ ;\alpha') = \phi\ (4r_h' G_i'/\mu_f;\ c_f \mu_f/k_f\ ;\alpha')$$

$$N_{St}' = \phi\ (N_{Re}'\ ;\ N_{Pr}\ ;\alpha')$$

The heat transfer data obtained for the wire screen matrices are shown graphically in Figures 1 thru 6 and are plotted as $N_{St}' N_{Pr}^{2/3}$ versus N_{Re}' for various porosities. Each plot shows the results of each of the three screen matrices assembled from one type of screen.

7. Description of Matrices.

The screen matrix is packed in such a way that the individual screens are arranged in parallel and in close contact with each other. The direction of the woven lattices of the screens are situated at random. The flow approaching and leaving the matrix is in the direction perpendicular to the screens. It is desirable that the test matrices be capable of exact geometric description, as regards surface area, volume of solids, diameters, etc., in order that the results may be put into forms which have general applicability. Consequently, matrices were chosen for which the geometry is completely controllable and yet which permit random three-dimensional flow which is characteristic of porous media. The reason for this particular choice is that wire screens permit a fairly wide variation of geometric parameters while retaining essentially the same type of flow passage geometry.

Test matrices were constructed from six different sizes of stainless steel wire screen. The table below summarizes the geometry of the test materials; the details of all matrices examined are given in Table I.

Screen	Nominal Mesh per inch	Nominal Wire Dia., In.	Screen Porosity = α
60 x 60 -.011	60 x 60	.011	.602
60 x 60 -.0075	60 x 60	.0075	.675
24 x 24 -.014	24 x 24	.014	.725
16 x 16 -.018	16 x 16	.018	.766
10 x 10 -.025	10 x 10	.025	.817
5 x 5 -.040	5 x 5	.040	.832

The screen matrices were all composed of circular sections of stainless steel wire screen having a diameter of six inches. For all the matrices tested each set consisted of three screens. Coppage's (2) data indicated that the number of screens had no affect on the convective heat transfer coefficient h. The prime consideration was to establish flow conditions which represented a true porous media. With such low flow rates (3 to 40 ft^3/hr), it was felt that these conditions were adequately met. All matrices were assembled in, and held in position during testing by a special matrix holding device described in Part III and shown in Figure 7.

An important assumption made in the analysis for the transient temperature technique used in this investigation, is that of adiabatic boundary conditions existing at the matrix boundaries. It is exceedingly difficult to provide adiabatic boundary conditions in a transient situation, since all insulating materials have some capacity for storing thermal energy. By using balsa wood for the matrix boundaries and for the entire test section as well, the heat transferred from the boundaries was held to a minimum. Locke (1) and Coppage (2) both point out the idealizations necessary in developing the experimental method used. From their analysis of heat loss to the boundaries they showed that the heat transferred from the boundaries to the screens was generally less than five percent of the storage capacity of the matrix up to the time of maximum slope.

8. Experimental Apparatus.

The apparatus assembled for this investigation is entirely different from that used by both Locke (1) and Coppage (2) in their projects. A flow diagram of the test system is shown in Figure 10. Basically the system consists of a balsa test section with a sliding drawer for holding the test matrix, an air metering device, an air ejector to provide flow thru the test core, a fan type blower, an air heater, a flow measuring system, and a temperature measuring system.

Ambient air is drawn through a 6 in. throat diameter, spun aluminum nozzle, by an air ejector system of a steam condensing plant. The nozzle was designed according to ASME specifications, contained in Reference (9), to insure smooth flow. The air then passes immediately into a 6 in. I. D. solid balsa test section. The test section is pictured in Figure 11. It is fitted with a sliding drawer which holds the three screen matrix. In all runs the orientation of the test apparatus is such that the incoming air flows vertically downward thru the nozzle and into the test section. The air passes thru the horizontal screen matrix and then past an air temperature thermocouple matrix $1\frac{1}{2}$ in. downstream from the screens. From there it flows through a piping arrangement into one of three Fischer-Porter flowrators. Flow rate is controlled by a 3/4 in. needle valve on the vacuum side of the flowrator. Fine control is afforded by a $\frac{1}{4}$ in. by-pass needle valve around the large needle valve. With a maximum fluid velocity thru the nozzle of about 1 ft/sec, uniformity of pressure over the matrix section is insured.

Adjacent to the test core is an air heating duct used for heating the screen matrix. The duct is an insulated L-shaped unit of circular cross-section, with a fan and heater located in the horizontal leg of the L.

This affords radiant shielding of the screen matrix thermocouples from the hot element of the heater. The duct is baffled in the vertical leg of the section of the unit in order to insure uniform air temperature discharging from the heater. The heating element and fan are individually controlled by two, 115 volt 60 cycle A.C., "Variacs" with a range of from 0 to 120 volts. Because of the low flow rates used in the heating duct and with the baffles installed, very little adjustment of the variacs was found necessary to maintain constant temperature air.

Temperature Measuring System. All thermocouples used are 24 gage Copper-Constantin. The flowrator temperature is measured by a mercury glass thermometer inserted downstream of the flowrators. The upstream ambient air temperature is measured by two thermocouples located on the circumference of the bell of the inlet nozzle. The downstream air temperature was measured by a matrix of five thermocouples. The entire downstream matrix consisted of thirteen thermocouples held in a frame and located in equal areas of the flow cross-section. A picture of the thermocouple matrix is shown in Figure 12. It was found that there was considerable temperature variation near the walls of the test section. In constant temperature tests run on this thermocouple array, the five central thermocouples, located in equal areas, gave excellent agreement. The outer two circles of thermocouples showed considerable variation, with the outermost circle giving the greatest deviation. The five central thermocouples in series, thus, were used, and measured the air temperature at the center of the core cross section.

The reference junctions were all placed in an ice bath at 32°F. The leads from the downstream air temperature matrix were led to a Leeds & Northrop, "Speedomax", Model G, emf recorder with a variable range of from 1 to 20 mv. The range selected for use on all runs was 0 - 2 mv. The

ambient air thermocouples were read with a Leeds & Northrup portable precision potentiometer. Provision was also made to insure uniform temperature of the screen matrix when heated in the air stream. Five thermocouples were welded to the screen matrix with a pencil point welder. These thermocouples were also located in equal areas of the cross section. Reference for this system was also an ice bath at 32°F and were read with a Leeds and Northrup portable precision potentiometer.

Sliding Drawer Matrix Holder. The experimental method requires that the test core be initially at a uniform temperature and that at the initial instant ($\theta = 0$) air at a different temperature enter the upstream side. This sudden change in conditions is accomplished by sliding the balsa drawer matrix holder out of the balsa test section and over a heated air supply until the temperature of the screens is uniform and at the desired temperature. The drawer is then pushed into the test section through which ambient air is flowing.

9. Experimental Procedure

The conditions of the idealized problem upon which the analysis is based must be duplicated. Ambient air is drawn through the inlet flow nozzle and allowed to flow through the test matrix while the flow rate is adjusted. After constant flow is established the sliding drawer containing the screens is pulled out and into the heated air stream. When the screens reach a steady state temperature, as indicated by monitoring thermocouples spotted onto the screens, the drawer is quickly inserted into the air stream and the experiment is started. The ambient air temperature is recorded, the initial screen temperature is recorded, and the transient downstream air temperature is recorded on the Leeds & Northrup "Speedomax" recorder. After the downstream air temperature has returned to nearly ambient air temperature, the run is terminated. No detectible variation in flow rate could be noticed throughout the runs. The flow induced by imposing a vacuum on the downstream side of the test section, is seemingly, an excellent method to obtain low controlled flow rates. Considerable trouble was experienced with unsteady and erratic flow patterns when induced flow was attempted with the suction side of a centrifugal blower attached to the test section. The extremely steady flow rate was not obtained until the vacuum system of the air ejector steam condenser was used.

The following data were recorded:

a. Atmospheric pressure

b. Atmospheric temperature

c. Initial matrix temperature (5 Copper-Constantin thermocouples)

d. Upstream ambient air temperature (2 Copper-Constantin thermocouples)

e. Downstream leaving air temperature as a function of time (5 Copper-Constantin thermocouples)

f. Flowrator temperature (Mercury thermometer)

10. Experimental Results.

The geometric specifications of all the screen matrices examined are tabulated in Table I. All the test data for the matrices are evaluated on the basis of the geometry of an individual screen. In other words, the matrices are packed in such a way that the total length of the matrix is equal to the individual screen thickness multiplied by the number of screens.

The experimental heat transfer performance is presented in Tables II to VII. The heat transfer data is also presented in graphical form by plotting $N_{St}' N_{Pr}^{2/3}$ versus N_{Re}' for various porosities as shown in Figures 1 through 6.

11. Discussion of Results

As described by previous investigators, heat transfer behavior of porous media, appears to follow, essentially, a single characteristic. In looking at the plots in Figures 1 to 6, Coppage's (2), data may quite satisfactorily be interpreted by straight lines drawn through the scatter. The general trend of the slope and position of the data is unmistakable. Slope and position of the lines show a definite increase with increasing porosity.

Coppage (2) pointed out that some degree of curvature is suspected in his results. This statement is based on the fact that some of his data were taken in the transition range of Reynolds numbers. Friction factor data which Coppage took, showed a non-linear increase of friction factor with decreasing Reynolds number. Since the friction factor is a measure of form drag and skin friction drag, an increase in this combined coefficient, indicates a transition effect. Skin friction is affected very much less than form drag since the growth of even small standing vortices behind bluff bodies has a greater effect on form drag than on skin friction drag. Therefore, because of the analogy between heat transfer and skin friction drag, discussed in Reference (10), the heat transfer data would be expected to be more linear than the friction factor data but still exhibit some small curvature. Coppage did not predict the degree of curvature because of the lack of data, but rather used a straight line representation. Equipped now with additional data in the lower Reynolds number range, it can be seen that this curvature actually does exist. In the plots in Figures 1 to 6, a proposed curvature is indicated which incorporates previous data with present data.

In the extremely low Reynolds number range, it was noticed that a very

definite increase in the value of h occured. The explanation afforded this result is that at some low Reynolds number, the value dependent upon screen porosity, the effect of natural convective cooling affects the forced convective cooling and causes unpredictable effects. The effects of this combined natural and forced convective cooling cannot be analyzed with the maximum slope technique used in this work. A technique for determining the natural convective cooling coefficient of porous media is certainly a problem which should be investigated. Since information is not available on this problem, no conclusions can be drawn from the results at these lowest Reynolds numbers.

It should be noted that in comparing data obtained in the lower three screen porosities, with Coppage's (2) data, the curves are either smoothly connecting or overlapping with each other. Only on the highest three porosities was there considerable variation in results, and then only in the vertical position of the curve. The general slope of the comparable section of the curve is approximately the same.

The data obtained will give only a slightly higher heat transfer coefficient h, than would result if the test section boundaries were truly adiabatic. This is because of the heat which will flow into the screens from the boundaries during a run. In order to minimize this, the test core and matrix holder were constructed of balsa wood, a material with very low heat capacitance. Romie (3) and Coppage (2) point out that experiments support the statement that gain of heat from the walls, has little effect when measurements taken at the flow center-line are used and when the maximum slope technique is used in determining NTU. To further minimize the effects of non-adiabatic boundaries, both of these techniques are incorporated in the testing procedure used.

12. Comparison of Present Data with Previous Results.

The heat transfer characteristics of square mesh screen matrices have been obtained over the Reynolds number range of 0.1 to 10.

Heat transfer results for various matrices are correlated on the basis of the effect caused by porosity and Reynolds number.

Previous data and present data agree quite well in their overlap region for the three lower porosity screens. There is a very definite curvature noted in the data as Reynolds number is reduced. There is no data available for comparison in the low Reynolds number range where this work was done, however it does follow a curved pattern as predicted by Coppage (2). The amount of curvature is unknown, therefore only a proposed curvature is indicated.

In the three highest porosity screens, vertical displacement of the curves occured. In the present data the value of $\underline{h}$ is somewhat higher than that shown by previous investigation. The possibility exists that in these higher porosity screens, a three screen matrix does not perform as a true porous media. It is possible, even with the very low flow rates, that there are insufficient obstructions to create the flow pattern required of a porous media. If this is true, then a higher heat transfer coefficient will probably result for the lower flow rates. Coppage (2) stated that a lower coefficient for the first screen in a matrix should be expected, thus yielding a slightly lower overall coefficient. However this appears to be true only at higher Reynolds numbers. At lower Reynolds numbers the opposite tendency seems to occur. Experiments with tube banks by Kays and Lo (11), show a definite tendency for $\underline{h}$ to be higher for the first row of tubes than for the subsequent rows. Using this geometry for comparison then, it is entirely possible for the results to vary in the manner they do.

13. Conclusions.

1. A testing technique has been developed for determining convective heat transfer data for air flow through wire screen matrices at low Reynolds numbers. The method is also useful for testing any core with high effectiveness at low Reynolds numbers.

2. Convective heat transfer data of square meshed, randomly packed screen matrices, composed of three screens, has been established for a range of porosities from 0.602 to 0.832 and for Reynolds numbers from 0.1 to 10.

3. Previous data for heat transfer to porous media are very limited in amount and non-existant over part of the Reynolds number range covered in this investigation. In the overlap region of data, excellent agreement was found in the three lowest porosity screens of the six sets of screens tested. However, further investigation is needed to substantiate the deviation of the present data from previous data in the three higher porosity matrices.

14. Recommendation for Future Work.

a. No data is yet available for porous media on the heat transfer coefficient due to natural convection. A technique is needed for obtaining such data.

b. Additional data is needed on the three matrices of highest porosity using more than three screens. This would verify whether the number of screens at the higher porosities have a significant effect on the heat transfer coefficient.

c. In the screens of 5 x 5 - 0.041 in. mesh, it was not possible to obtain heat transfer coefficients for N_{Re}' below 16. The erratic nature of the cooling curves was so severe that it was impossible to use them for data. Use of additional number of screens in the matrix should give a much smoother response and enable extension of this matrix data to a much lower value of N_{Re}'.

d. The analysis of the heat transfer coefficient of these screens by using the time temperature history of the screens, would afford an excellent check on the results of all the previous investigations. This could be accomplished by attaching a series of thermocouples to the screen wires by minute spot welding, and monitoring their time-temperature behavior. Analysis of the data could be done by the thermal capacitance technique.

BIBLIOGRAPHY

1. G. L. Locke, "Heat Transfer and Flow Friction Characteristics of Porous Solids," Technical Report No. 10, Navy Contract N6-ONR-251 Task Order 6, Stanford University, 1 June, 1950.

2. J. E. Coppage, "Heat Transfer and Flow Friction Characteristics of Porous Media," Technical Report No. 16, Navy Contract N6-ONR-251 Task Order 6, Stanford University, 1 December, 1952.

3. R. E. Romie, et al, "Heat Transfer and Pressure Drop Characteristics of Four Regenerative Heat Exchanger Matrices," ASME Paper No. 51-SA-34, presented to Semi-Annual Meeting, Toronto, Ontario, Canada, June 1951.

4. T. E. W. Schumann, "Heat Transfer: A Liquid Flowing Through a Porous Prism," Journal of the Franklin Institute, Vol. 208, p. 405 (1929).

5. C. C. Furnas, "Heat Transfer From a Gas Stream to a Bed of Broken Solids," U. S. Bureau of Mines Bulletin No. 361 (1932).

6. O. A. Saunders and H. Ford, "Heat Transfer in the Flow of Gas Through a Bed of Solid Particles," Journal of the Iron and Steel Institute, Vol. 141, p. 291 (1940).

7. G. O. A. Lof and R. W. Hawley, "Unsteady-State Heat Transfer Between Air and Loose Solids," Industrial and Engineering Chemistry, Vol. 40, p. 1061 (1948).

8. O. A. Saunders and S. Smoleniec, "Heat Transfer in Regenerators," paper presented at the General Discussion on Heat Transfer, London, Sept. 1951, Section V, 6th paper.

9. Report of A. S. M. E. Special Research Committee on Fluid Meters, "Fluid Meters, Their Theory and Application, Part I, Fourth Edition, 1937.

10. O. P. Bergelin, A. P. Colburn, and H. L. Hull, "Heat Transfer and Pressure Drop During Viscous Flow Across Unbaffled Tube Banks," University of Deleware Engineering Experiment Station, Newark, Deleware, June 1950.

11. W. M. Kays and R. K. Lo, "Basic Heat Transfer and Flow Friction Design Data for Gas Flow Normal to Banks of Staggered Tubes - Use of a Transient Technique," Technical Report No. 15, Navy Contract N6-ONR-251 Task Order 6, Stanford University, August 15, 1952.

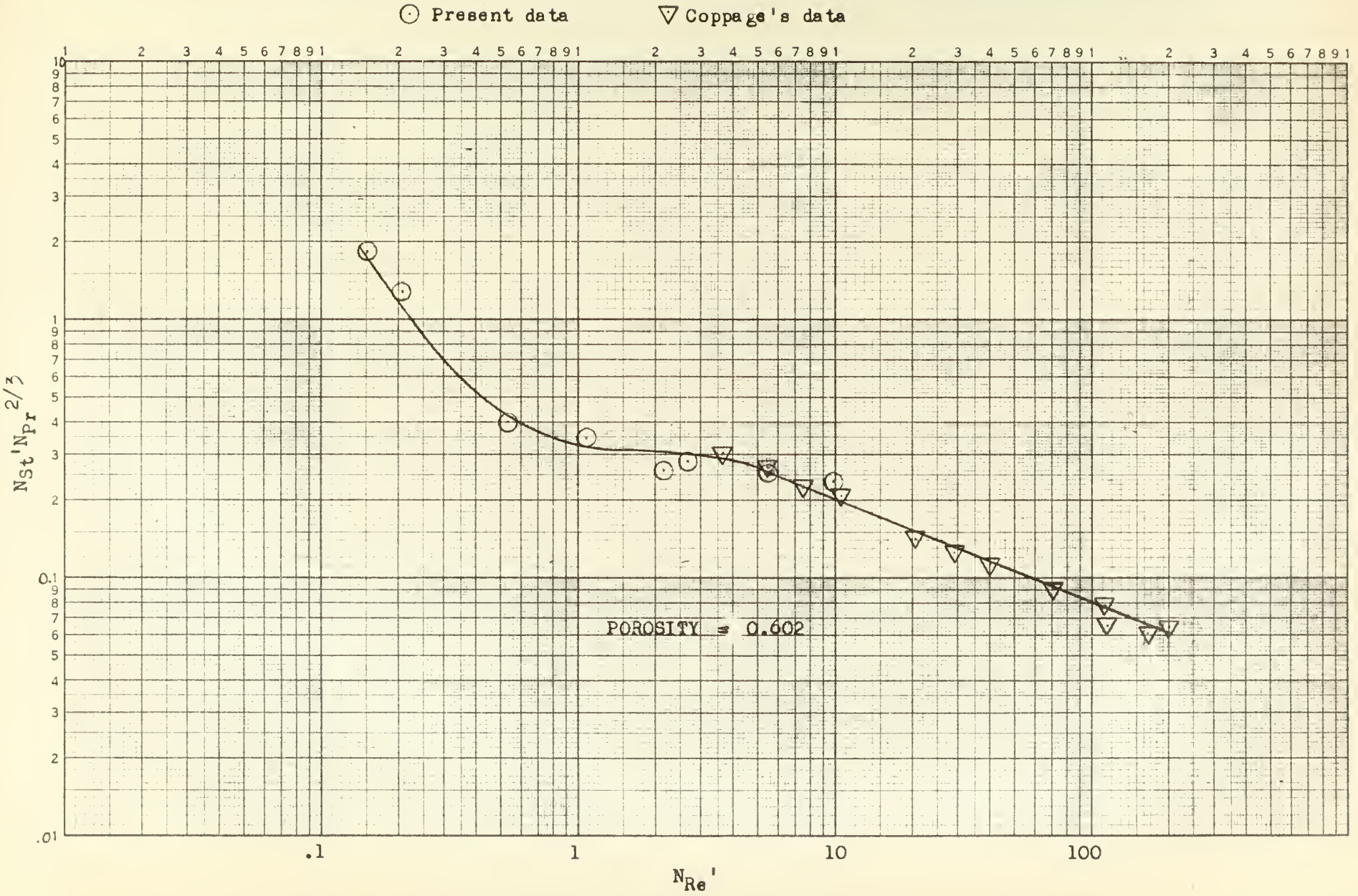

$N_{St}'N_{Pr}^{2/3}$ versus N_{Re}' for the 60 x 60 mesh per inch --0.011 inch wire diameter

Figure 1

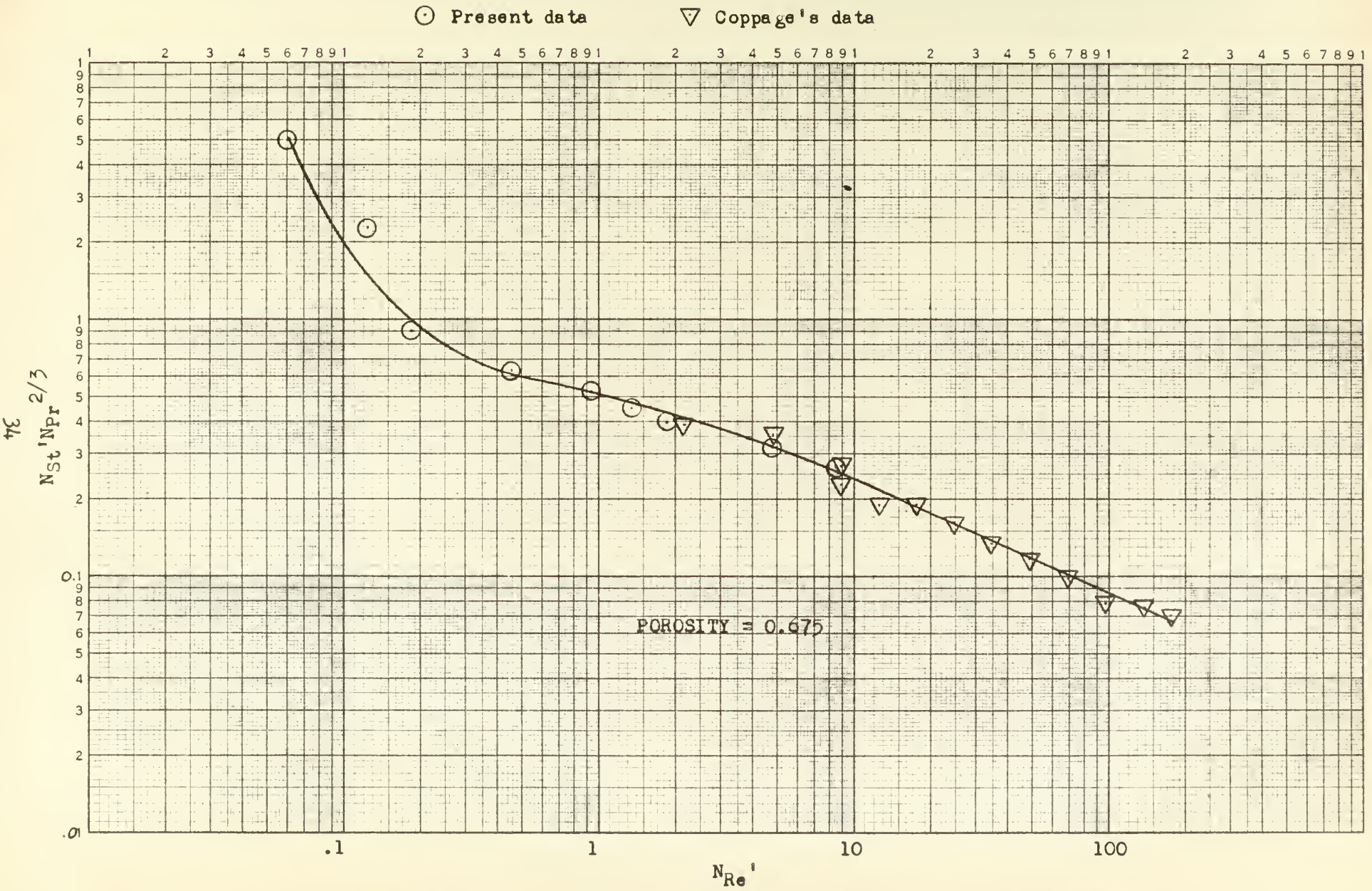

$N_{St}'N_{Pr}^{2/3}$ versus N_{Re}' for the 60 x 60 mesh per inch --0.0075 inch wire diameter

Figure 2

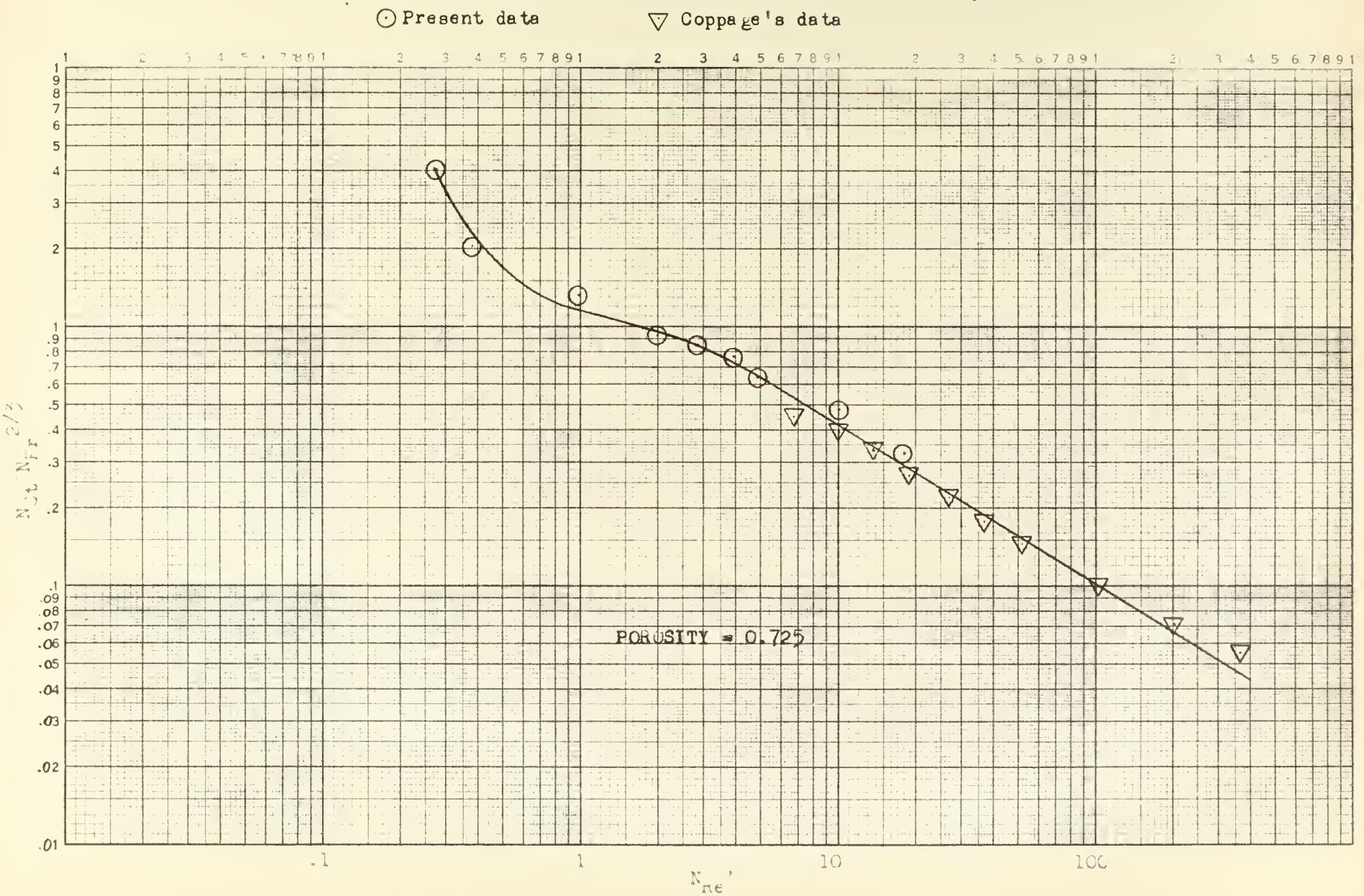

$N_{St} N_{Pr}^{2/3}$ versus N_{Re} for the 24 x 24 mesh per inch - 0.014 inch wire diameter

Figure 3

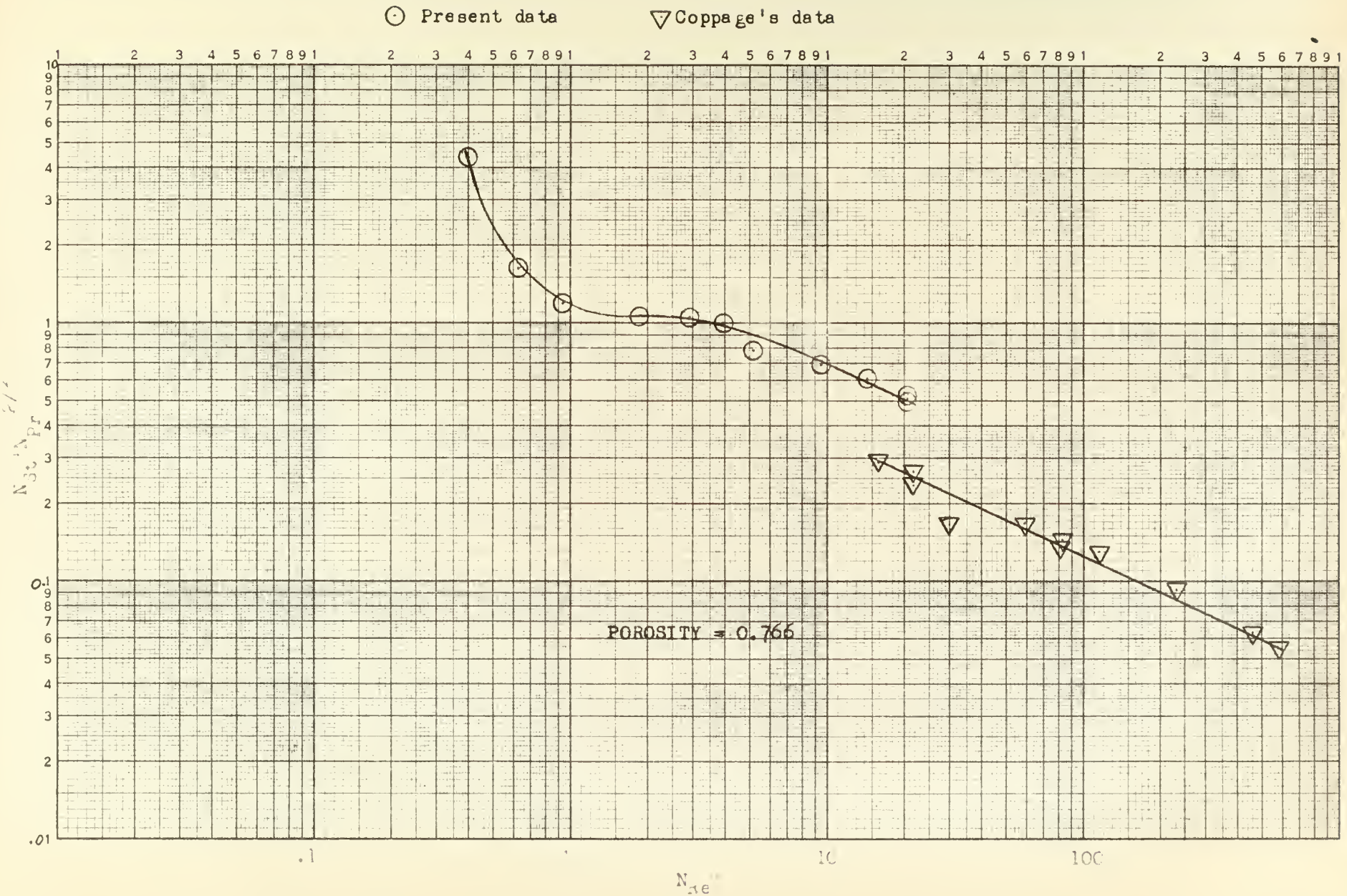

$N_{St}{N_{Pr}}^{2/3}$ versus N_{Re}' for the 16 x 16 mesh per inch - 0.018 inch wire diameter

Figure 4

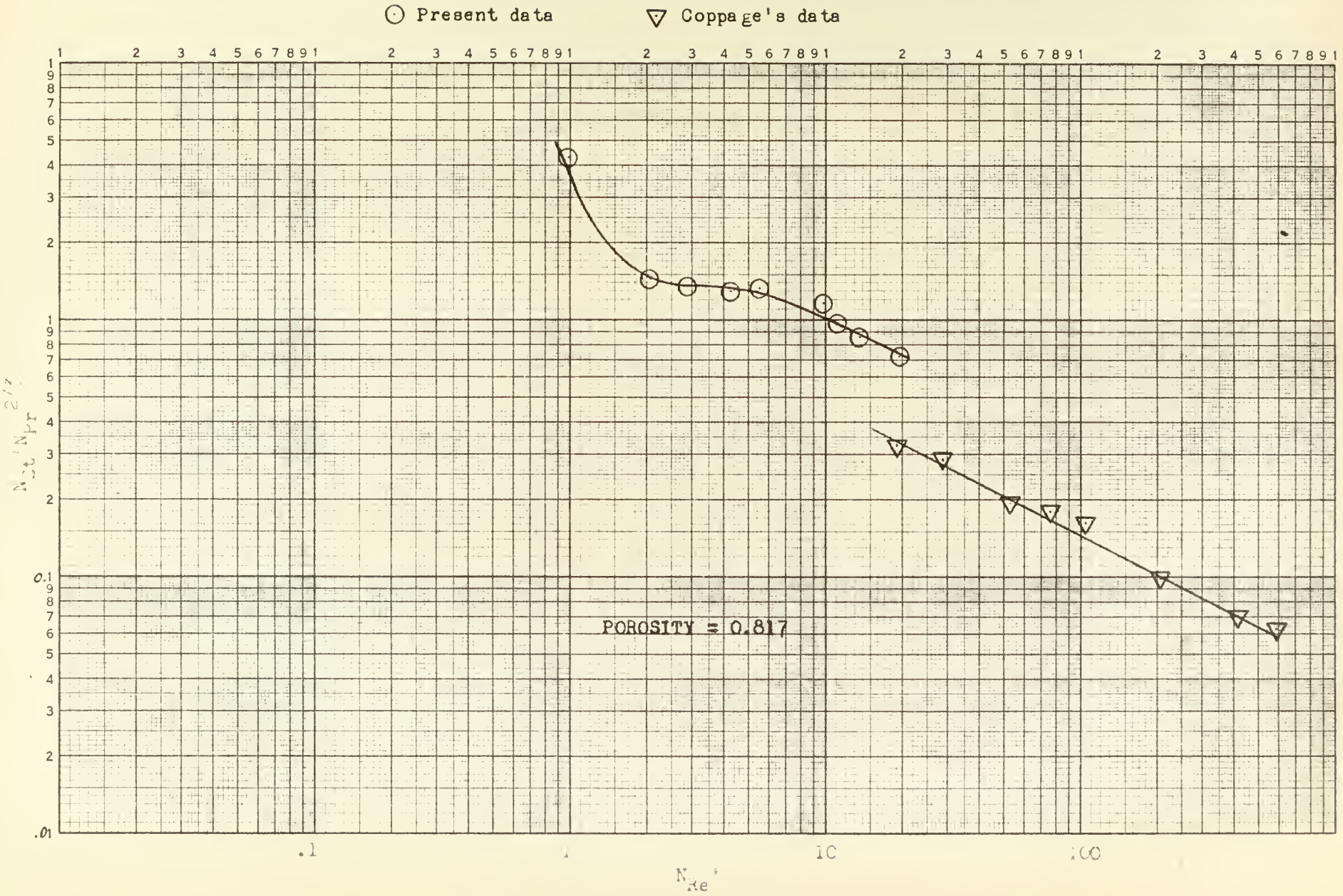

$N_{St} N_{Pr}^{2/3}$ versus N_{Re}' for the 10 x 10 mesh per inch -- 0.025 inch wire diameter

Figure 5

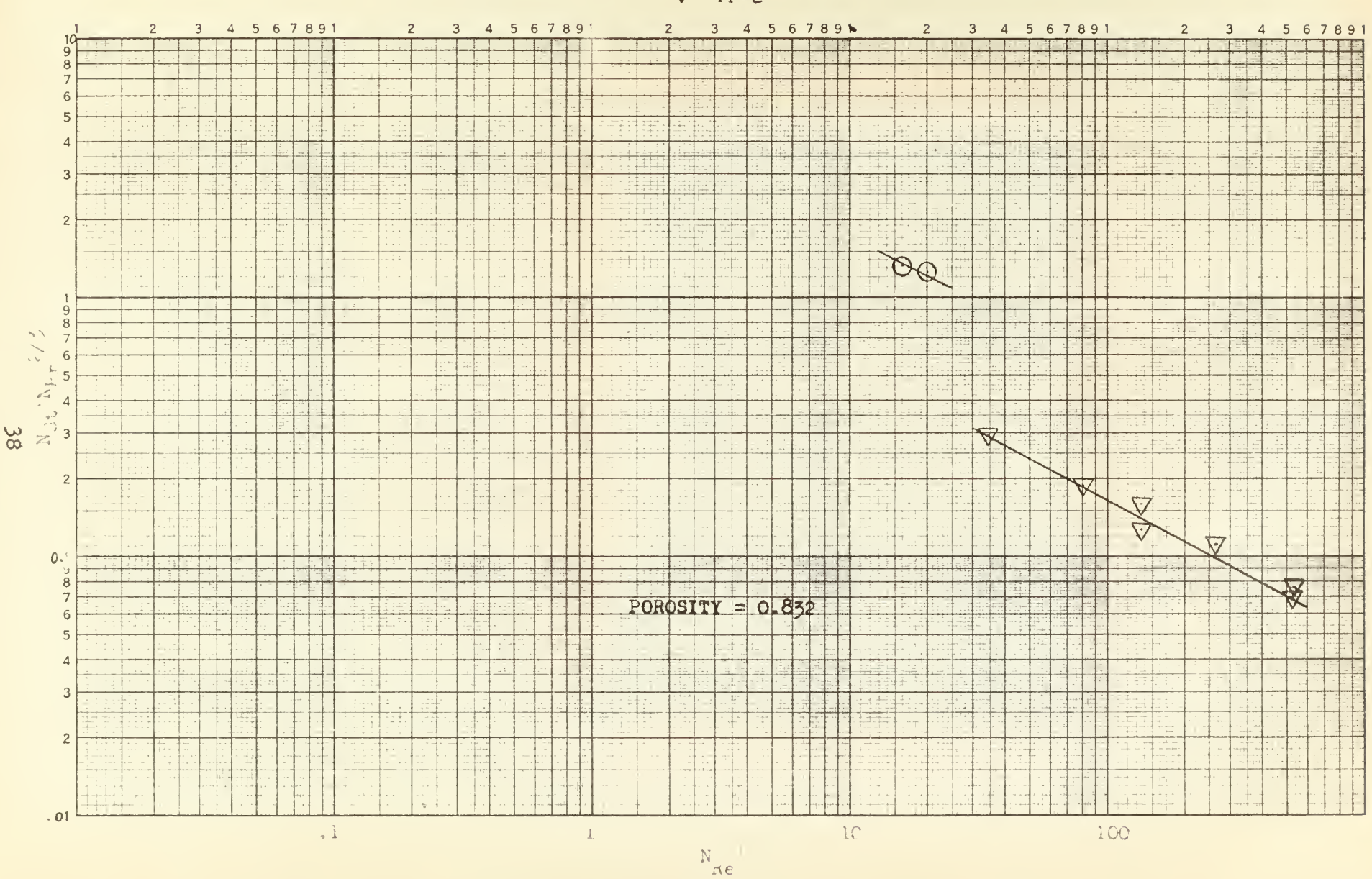

$N_{St}\,'N_{Pr}^{2/3}$ versus N_{Re}' for the 5 x 5 mesh per inch -- 0.041 inch wire diameter

Figure 6

Photo shows the sliding drawer matrix holder. The test screens are mounted in the drawer and held in place by a balsa frame. To the left of the drawer can be seen the test screens with thermocouples welded to them for measuring the initial screen temperature.

Figure 7

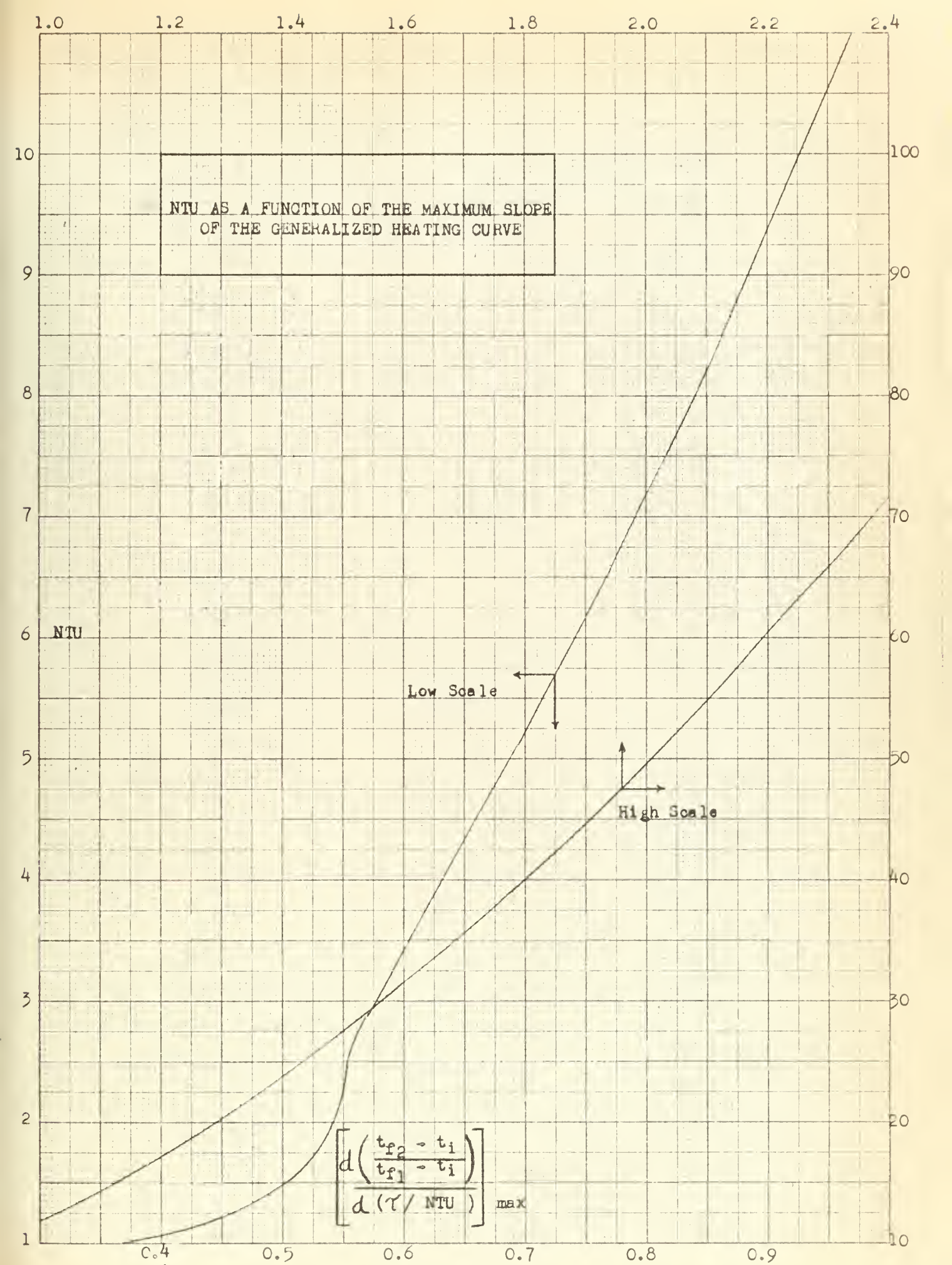
NTU AS A FUNCTION OF THE MAXIMUM SLOPE
OF THE GENERALIZED HEATING CURVE
NTU
Low Scale
High Scale
$\left[\frac{d\left(\frac{t_{f_2} - t_i}{t_{f_1} - t_i}\right)}{d(\tau / NTU)}\right]_{max}$
1.0
1.2
1.4
1.6
1.8
2.0
2.2
2.4
0.4
0.5
0.6
0.7
0.8
0.9
1
2
3
4
5
6
7
8
9
10
10
20
30
40
50
60
70
80
90
100

Figure 8

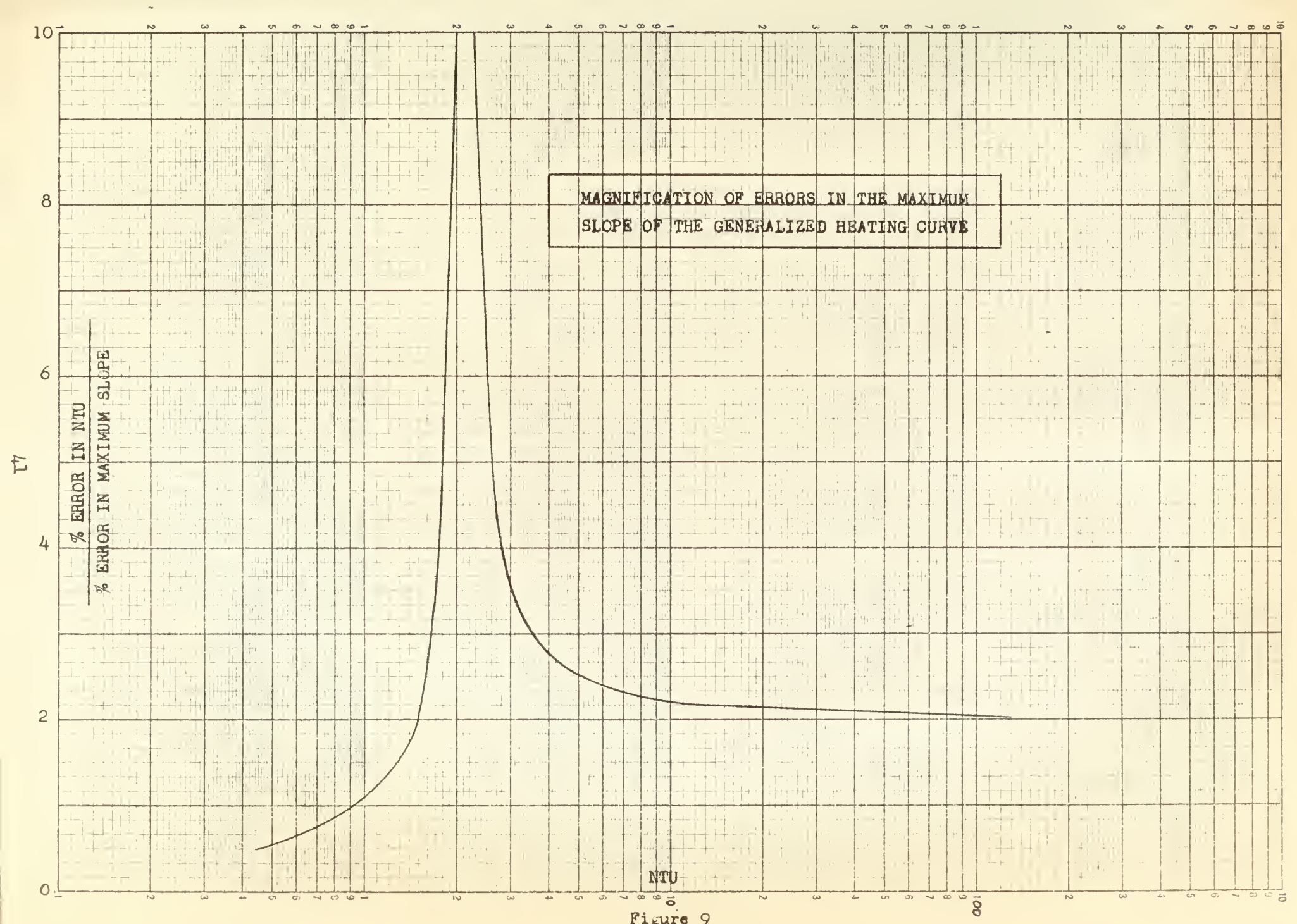
MAGNIFICATION OF ERRORS IN THE MAXIMUM SLOPE OF THE GENERALIZED HEATING CURVE
% ERROR IN NTU
% ERROR IN MAXIMUM SLOPE
T7
NTU
10
8
6
4
2
0
1
2
3
4
5
6
7
8
9
10
100

Figure 9

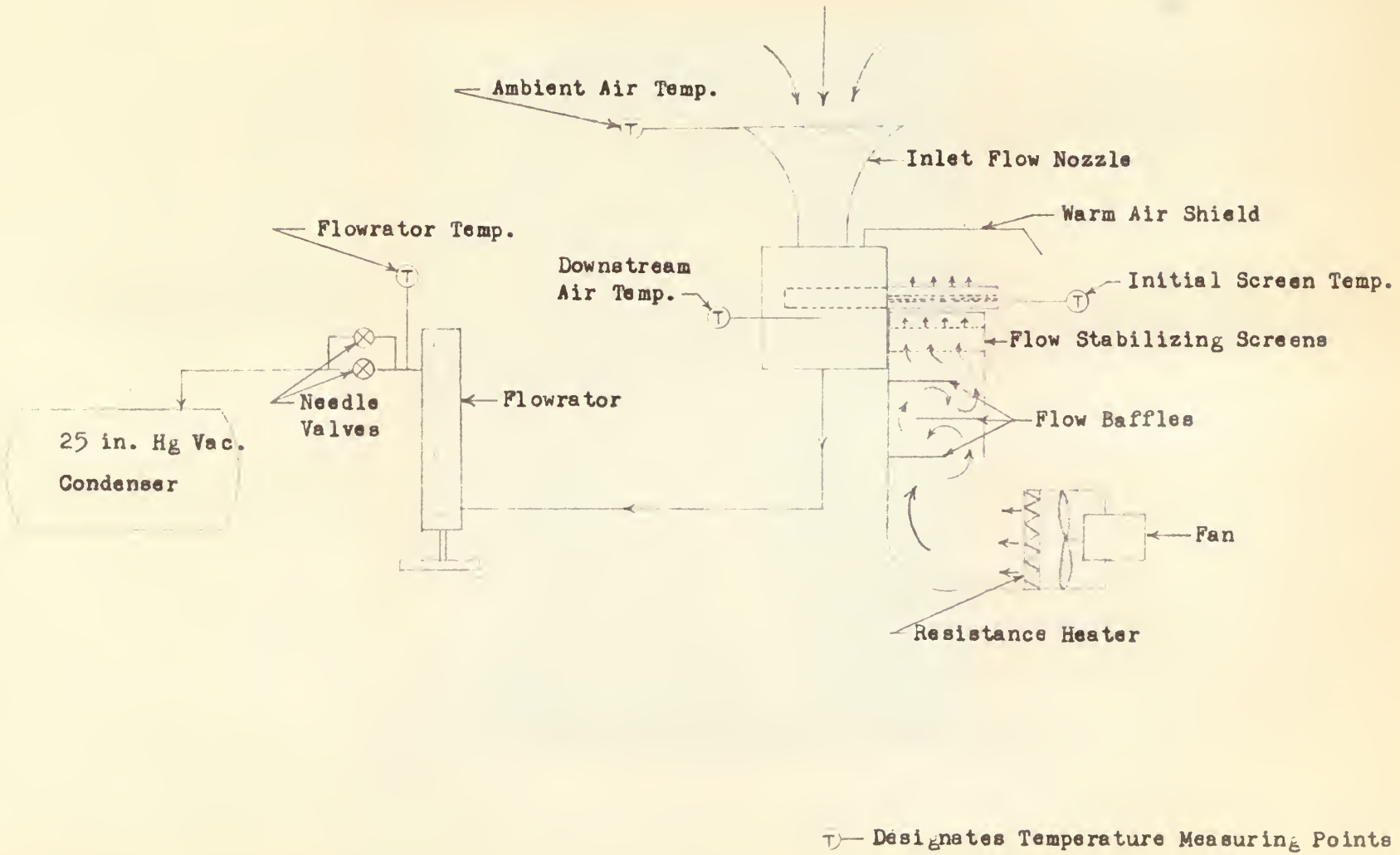

Flow Diagram of Test Apparatus

Figure 10

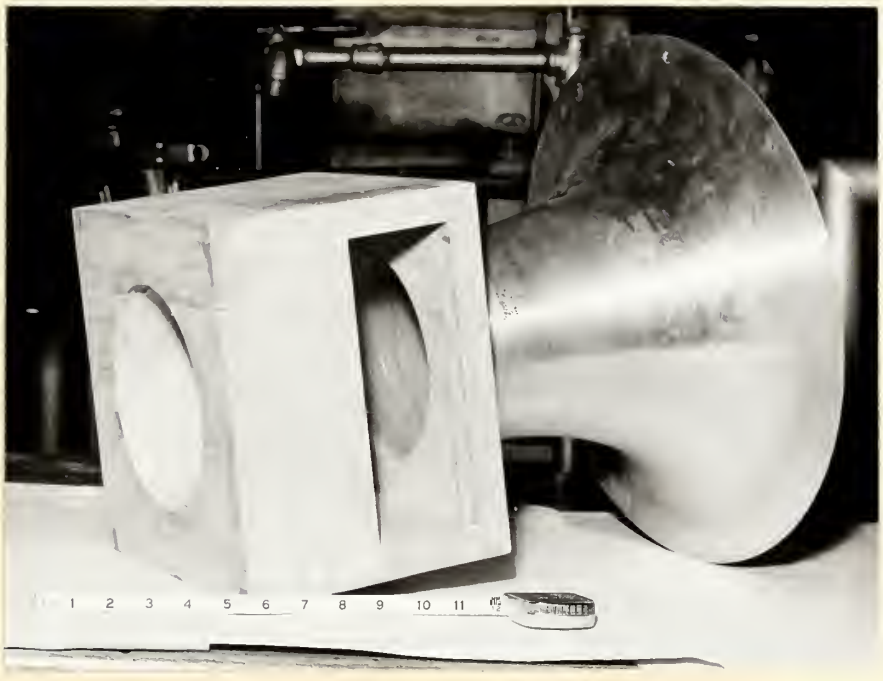

Photo shows the path traveled by air as it flows through and inlet nozzle and into the test core. Rectangular opening accommodates the sliding drawer which holds the screen matrix to be tested.

Figure 11

Photo showing the thermocouple matrix consisting of thirteen thermocouples which could be read either individually or in series. Thermocouple leads were brought out of the edge of the drawer and into a selector switch.

Figure 12

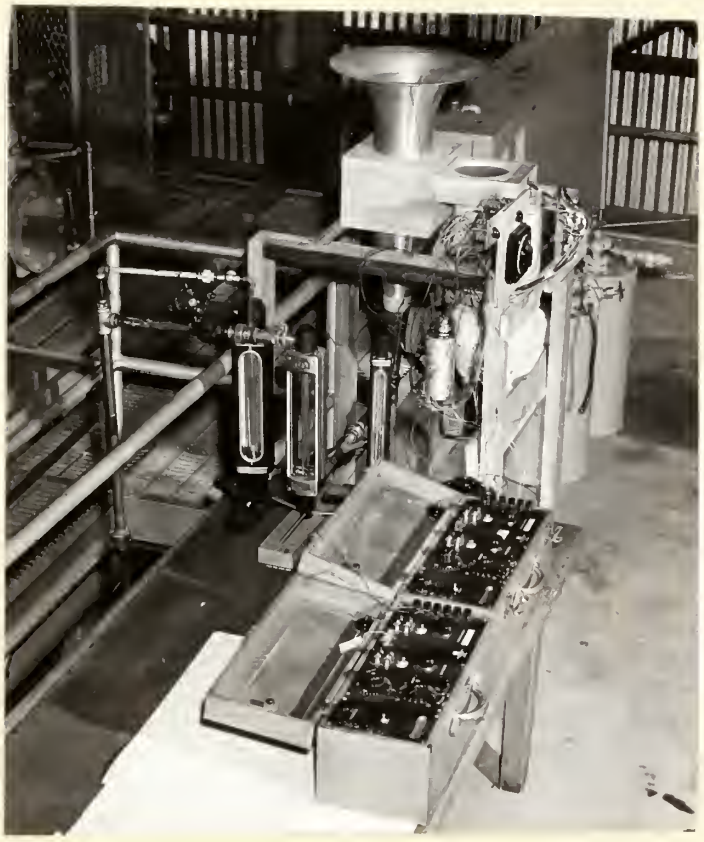

Photo shows the orientation of the test cell for all runs. The sliding drawer is resting over the warm air duct in the position required for heating the screens. The potentiometers were used to measure the ambient air and the initial screen temperature. The continuous pen recorder which was used to record the temperature-time history of the downstream air, is not shown.

Figure 13

TABLE I

DETAILS OF WIRE SCREENS USED IN MATRICES

Screen Size	60 x 60 -0.011	60 x 60 -0.0075	24 x 24 -0.014	16 x 16 0.018	10 x 10 0.025	5 x 5 0.041
Nominal Mesh/Inch	60 x 60	60 x 60	24 x 24	16 x 16	10 x 10	5 x 5
Nominal Wire Dia., In.	0.011	0.0075	0.014	0.018	0.025	0.041
Actual Wire Dia., In.	0.0106	0.0075	0.0136	0.0177	0.0245	0.0405
Frontal Area A_t, ft^2	0.1962	0.1962	0.1962	0.1962	0.1962	0.1962
Length of Matrix, ft	0.00754	0.00415	0.00645	0.00858	0.0125	0.0182
Mass W_s', lbm	0.123	0.0653	0.0873	0.0962	0.118	0.150
Porosity α'	0.602	0.675	0.725	0.766	0.817	0.832
Heat Transfer Area, A', ft^2	0.848	0.582	0.408	0.343	0.305	0.254
Heat Transfer area/unit vol. β', ft^2/ft^3	1815	2090	980	623	352	196
Hydraulic Radius r_h', ft x 10^4	3.32	3.23	7.40	12.3	23.2	42.5
Free Flow Area $A_f' = \alpha' A_t$, ft^2	0.118	0.132	0.142	0.150	0.160	0.163

Note: For all screens, material is 18/8 stainless steel, specific heat .12 BTU/lbm°F; thermal conductivity, 10 BTU/hr ft^2 °F/ft; density, 490 lbm/ft^3. Parameters are computed for a single screen.

TABLE II

HEAT TRANSFER DATA

60 x 60 MESH PER INCH - 0.011 INCH WIRE DIAMETER SCREEN POROSITY - 0.602

No. of Screens	Run	w_f lbm/hr	G_i' lbm/hr ft^2	t_i °F	t_{f_1} °F	NTU	h BTU/hr ft^2°F	N_{Re}'	$N_{St}'N_{Pr}^{2/3}$
3	1	39.4	402	100.72	61.05	6.4	23.77	9.78	0.236
3	2	22.25	113	102.35	61.00	7.0	14.68	5.52	0.258
3	3	10.72	54.7	100.23	61.42	7.65	7.73	2.66	0.282
3	4	8.65	44.1	102.25	61.42	7.05	5.75	2.14	0.261
3	5	4.37	22.3	104.60	60.88	9.35	3.86	1.09	0.345
3	6	2.14	10.9	103.95	61.68	10.85	2.19	0.531	0.401
3	7	0.84	4.28	103.20	60.79	35.0	2.77	0.208	1.29
3	8	0.61	3.11	104.85	61.23	49.5	2.85	0.152	1.83

TABLE III

HEAT TRANSFER DATA

60 x 60 MESH PER INCH - 0.0075 INCH WIRE DIAMETER SCREEN POROSITY - 0.675

No. of Screens	Run	w_f lbm/hr	G_i' lbm/hr ft^2	t_i °F	t_{f_1} °F	NTU	h BTU/hr ft^2°F	N_{Re}'	$N_{St}'N_{Pr}^{2/3}$
3	1	39.4	402	101.95	75.2	4.45	23.85	8.44	0.266
3	2	22.25	113	102.20	75.4	5.30	16.20	4.77	0.319
3	3	8.65	44.1	102.30	75.1	6.60	7.84	1.86	0.398
3	4	6.26	31.9	102.20	75.0	7.05	6.07	1.34	0.425
3	5	4.38	22.3	102.40	79.3	8.65	5.21	0.940	0.522
3	6	2.14	10.9	103.25	79.7	10.45	3.08	0.460	0.630
3	7	0.865	4.41	102.70	80.1	15.02	1.79	0.185	0.906
3	8	0.611	3.11	99.60	74.35	35.70	3.18	0.125	2.28
3	9	0.306	1.56	101.75	75.20	83.00	3.50	0.061	5.01

TABLE IV

HEAT TRANSFER DATA

24 x 24 MESH PER INCH - 0.014 INCH WIRE DIAMETER SCREEN POROSITY - 0.725

No. of Screens	Run	w_f lbm/hr	G_i' lbm/hr ft^2	t_i ^oF	t_{f_1} ^oF	NTU	h BTU/hr ft^2 ^oF	N_{Re}'	$N_{St}'N_{Pr}^{2/3}$
3	1	39.4	402	102.65	69.30	3.55	27.42	18.0	0.325
3	2	22.25	113	100.90	68.90	5.20	22.70	10.2	0.481
3	3	10.72	54.7	101.60	70.75	6.90	14.52	4.90	0.638
3	4	8.65	44.1	101.90	70.70	8.30	14.10	3.95	0.769
3	5	6.27	31.9	99.25	70.70	9.15	11.25	2.86	0.846
3	6	4.37	22.3	100.50	71.30	10.1	8.66	1.99	0.935
3	7	2.16	11.0	102.20	72.7	14.4	6.11	0.99	1.335
3	8	0.84	4.28	102.80	72.5	22.45	3.70	0.38	2.07
3	9	0.611	3.11	102.00	71.2	27.4	3.28	0.28	4.01

TABLE V

HEAT TRANSFER DATA

16 x 16 MESH PER INCH - 0.018 INCH WIRE DIAMETER SCREEN POROSITY - 0.766

No. of Screens	Run	w_f lbm/hr	G_i' lbm/hr ft^2	t_i ^oF	t_{f_1} ^oF	MTU	h BTU/hr ft^2 ^oF	N_{Re}'	$N_{St}' N_{Pr}^{2/3}$
3	1	28.05	143	100.22	74.66	4.35	28.40	20.4	0.505
3	2	28.05	143	102.35	73.68	4.55	29.70	20.4	0.522
3	3	19.74	100.8	104.75	73.60	5.30	24.40	14.4	0.615
3	4	12.97	66.1	102.70	73.63	5.95	17.98	9.44	0.690
3	5	7.13	36.4	102.47	72.97	6.35	11.20	5.18	0.781
3	6	5.36	27.3	103.11	70.15	8.60	10.72	3.90	0.996
3	7	4.02	20.4	104.95	69.80	9.05	8.47	2.93	1.05
3	8	2.59	13.2	102.70	67.64	9.25	5.58	1.89	1.07
3	9	1.30	6.63	101.90	66.35	10.30	3.11	0.945	1.19
3	10	0.865	4.41	101.55	66.21	14.1	2.84	0.630	1.63
3	11	0.550	2.80	99.88	65.95	36.25	4.64	0.400	4.2

TABLE VI

HEAT TRANSFER DATA

10 x 10 MESH PER INCH - 0.025 INCH WIRE DIAMETER SCREEN POROSITY - 0.816

No. of Screens	Run	w_f lbm/hr	G_i' lbm/hr ft^2	t_i ^oF	t_{f_1} ^oF	NTU	h BTU/hr ft^2 ^oF	N_{Re}'	$N_{St}'N_{Pr}^{2/3}$
3	1	15.14	77.3	98.98	71.12	5.2	20.65	19.5	0.725
3	2	10.72	54.7	99.27	72.62	6.6	16.12	13.8	0.858
3	3	8.65	44.1	99.45	72.00	7.0	15.90	11.1	0.976
3	4	7.61	38.8	101.72	72.48	8.4	16.75	9.81	1.17
3	5	4.28	21.8	101.59	72.93	9.6	10.79	5.52	1.335
3	6	3.20	16.3	101.72	73.68	9.35	7.85	4.13	1.305
3	7	2.25	11.5	101.64	73.42	9.85	5.82	2.90	1.370
3	8	1.60	8.15	102.00	73.95	10.05	4.42	2.06	1.465
3	9	0.764	3.89	100.84	73.42	31.00	6.21	0.985	4.320

TABLE VII

HEAT TRANSFER DATA

5 x 5 MESH PER INCH - 0.041 INCH WIRE DIAMETER SCREEN POROSITY - 0.832

No. of Screens	Run	w_f lbm/hr	G_i' lbm/hr ft^2	t_i ^oF	t_{f_1} ^oF	NTU	h BTU/hr ft^2 ^oF	N_{Re}'	$N_{St}'Pr^{2/3}$
3	1	8.65	44.1	101.90	71.80	7.40	20.2	20.0	1.26
3	2	6.92	35.3	102.39	71.98	7.75	16.9	16.0	1.32